Materials Physics and Chemistry (2019) Volume 1, No 3
doi:10.18282/mpc.v1i3.584

Original Research Article

Role of Oxygen Pressure on the Surface Properties of Polycrystalline Cu_2O Films Deposited by Thermal Evaporator

I. A. Khan[1], S. A. Hussain[1], A. S. Nadeem[1], M. Saleem[2], A. Hassnain[3], R. Ahmad[3]*

[1] Department of Physics, Government College University Faisalabad, 38000 Faisalabad, Pakistan
[2] Department of Physics, Lahore University of Management Sciences, Lahore 54000, Pakistan
[3] Department of Physics, Government College University Lahore, 54000 Lahore, Pakistan
**Correspondence: ejaz_phd@yahoo.com*

ABSTRACT

Polycrystalline cuprous oxide (P-Cu_2O) films are deposited on Cu substrates for various (0.2, 0.3 and 0.4 mbar) oxygen pressures (OP) by thermal evaporator. The XRD pattern shows the development of Cu (200), Cu_2O (200) and Cu_2O (311) diffraction planes which confirms the deposition of P-Cu_2O films. The intensity of Cu_2O (200) and Cu_2O (311) planes is associated with the increase of OP. The crystallite size and microstrains developed in (200) and (311) planes are found to be 19.31, 21.18, 11.32 nm; 22.04, 23.11, 12.08 nm and 0.113, 0.103, 0.193; 0.099, 0.096, 0.181 with increasing OP respectively. The d-spacing and lattice constant are found to be 0.210, 0.128 nm and 0.421, 0.425 nm respectively. The bond length of P-Cu_2O film is found to be 0.255 nm. The crystallites/unit area of these planes is found to be 12.21, 7.46, 45.16 nm^{-2} and 8.21, 5.75, 37.16 nm^{-2} respectively. The texture coefficients of these planes are found to be 1.22, 1.26, 1.11 and 0.78, 0.74 and 0.56 with increasing OP respectively. The O and Cu contents are found to be 5.31, 5.92, 6.94 wt % and 83.01, 82.44, 80.65 wt % respectively. The thickness and growth rate of P-Cu_2O films are found to be 87.9, 71.9, 65.5 nm and 17.6, 14.2, 13.1 (nm/min) with increasing OP respectively. The SEM micro-structures reveal the formations of patches of irregular shapes, rounded nano-particles, clouds of nano-particles and their distribution depend on the increasing OP. The refractive index and energy band gap of P-Cu_2O films are found to be 1.96, 1.89, 1.92 and 2.47, 2.44 and 2.25 eV with increasing OP respectively.

Keywords: *Weight Fraction; Film Thickness; Energy Band Gap; Crystallites; Lattice Parameters; SEM*

Received: Jun 14, 2019 **Accepted:** Aug 7, 2019 **Online:** Aug 24, 2019

1. Introduction

Copper oxide films have attracting huge attention as an important semiconducting material because of their outstanding applications in solar cells, magnetic storage devices, photoelectrochemical cells, catalysts for water splitting, gas sensor, biosensors and electrode material for lithium ion battery. Copper being multivalent, it forms many oxides, among them; cupric oxide (CuO) and cuprous oxide (Cu_2O) films are well known p-type semiconducting materials. The CuO and Cu_2O materials show different crystal structures; CuO has monoclinic crystalline structure with lattice parameters a = 0.468 nm, b = 0.342 nm, c = 0.513 nm whereas Cu_2O has cubic crystalline structure with lattice parameter a = 0.427 nm. It is known that the energy band gap (2.1 eV) of Cu_2O film is greater than the energy band gap (1.21-1.51 eV) of CuO film. The remarkable properties of Cu_2O films which make it suitable for the deposition of thin film solar cells are cellular inertness, good carrier mobility, relatively high minority carrier diffusion length, high optical absorption coefficient, high transparency, non-toxic, high energy band gap in the visible region and better electrical response[1-8]. The CuO or Cu_2O films are being deposited through various routes like DC and RF sputtering, sol-gel, electrodeposition, chemical vapor deposition, pulsed laser deposition, thermal evaporation and plasma evaporation have been used to deposit Cu_2O films on various substrates[9-19]. In the present work, thermal evaporator is used to deposit Cu_2O films because thermal evaporator is cost effective and simple route to deposit such type of important material in the form of thin films.

The polycrystalline cuprous oxide (P-Cu_2O) films are deposited on Cu substrates for various (0.2, 0.3 and 0.4 mbar) oxygen pressure (OP) by thermal evaporator while the other deposition parameters like the boat temperature (800 °C), source to substrate distance (2 cm) and the deposition time (5 min) remain constant. The deposited P-Cu_2O films are characterized by using X-ray diffraction (XRD), scanning electron microscopy (SEM), energy dispersive X-ray spectroscopy (EDX) and ellipsometric spectroscopy (ES) in order to study the crystal structure, crystallinity, crystallite size, dislocation density, micro-strains, lattice parameters, unit cell volume, texture coefficient, number of crystallites/unit area, surface morphology, shape, size and distribution of nano-particles, elemental analysis, absorption coefficient, refractive index and energy band gap respectively.

2. Experiment

The P-Cu_2O films are deposited on Cu substrates for various (0.2, 0.3 and 0.4 mbar) OP by thermal evaporator. **Figure 1** shows the schematic diagram of thermal evaporator used to deposit P-Cu_2O films. The detailed information about the locally available thermal evaporator is found in literature[20], however, in this experiment, the conventional heater and thermal evaporator plate are replaced by power supply and tungsten boat respectively. A power supply is used to provide current to tungsten boat and hence temperature. The solid Cu (purity 99.9%) is polished with SiC abrasive papers of different grids, washed with acetone to remove the contamination and then placed inside the tungsten boat as a source material whereas the Cu substrates are placed at 2 cm in front of tungsten boat.

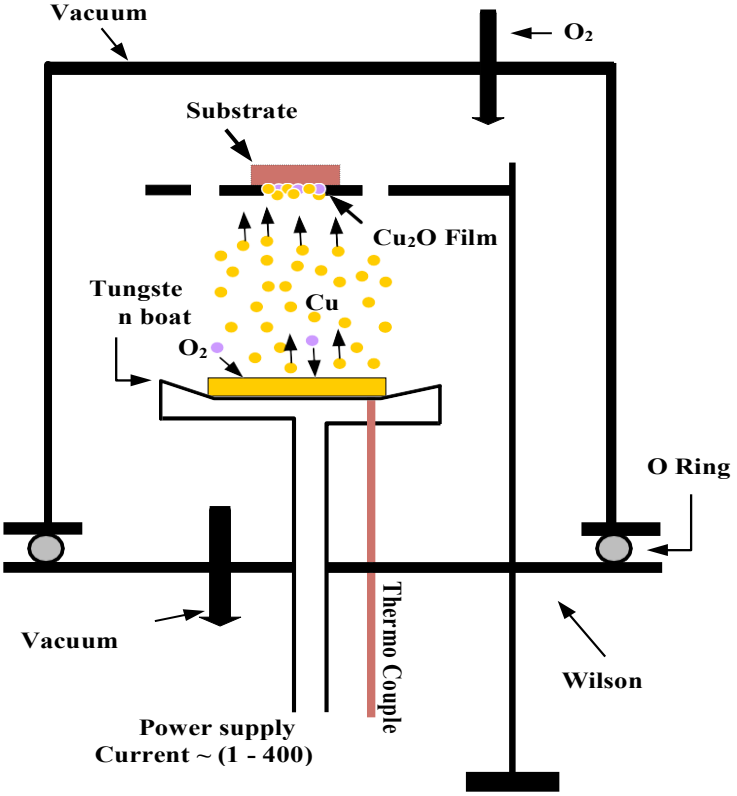

Figure 1. Schematic illustration of thermal evaporator**.**

The vacuum chamber is evacuated down to the pressure of 10^{-2} mbar with the help of rotary pump and is filled with oxygen gas up to the desire (0.2, 0.3, 0.4 mbar) OP. The basic mechanism behind the formation of P-Cu_2O films on Cu substrates is as follows: the solid Cu placed inside the tungsten boat gets sufficient amount of energy results in its evaporation in the form of atoms, molecules or ions which travels through the oxygen environment towards the substrate surface. The evaporated Cu species may or may not react with oxides to form copper oxide depending on the energy of oxides and evaporated Cu species. We hypothesize that the evaporated Cu species are of different kinds according to their energies. The higher energy Cu species may reach at the substrate surface without making any reaction with the oxides and deposit on the substrate surface in the form of layer. The lower energy Cu species have sufficient time during their travelling and may react with oxides to form copper oxide which is deposited on the substrate surface in the form of layer. Keep in mind, the energy of the evaporated Cu and newly formed copper oxide phase are decreased with the increase of OP.

3. Results and Discussions

3.1 Elemental Composition, Thickness and Growth Rate of Films

The ES technique is used to estimate the film thickness and growth rate of P-Cu_2O films deposited for 0.2, 0.3, and 0.4 mbar OP. The growth rate (nm/min) is the ratio of film thickness to the deposition time[20]. **Figure 2** demonstrates the variation of film thickness and growth rate of P-Cu_2O films as a function of OP. The film thickness and growth rate of P-Cu_2O films are found to be 87.9, 71.9, 65.5 nm and 17.6, 14.2, 13.1 (nm/min) for various OP respectively. It means that the film thickness and growth rate are decreased with the increase of OP. It is known that the collisions between the involved species increase with the increasing OP. The increasing collisions will decrease the energy of the involved and hence flux which in turn decrease the deposition rate and hence film thickness and growth rate.

Figure 3 shows the elemental composition of O and Cu in the P-Cu_2O films deposited for various (0.2, 0.3 and 0.4 mbar) OP. The elemental composition of O and Cu are found to be ~5.31, ~5.92, ~6.94 wt % and ~83.01, ~82.44, ~80.65 wt % when the P-Cu_2O films are deposited for various OP respectively. The greater Cu content indicates the deposition of Cu-rich P-Cu_2O films. Figure3 reveals that the amount of Cu in the deposited films is decreased with the increase of OP while the amount of O is increased with the increase of OP. The decreasing amount of Cu indicates that the film thickness is increased.

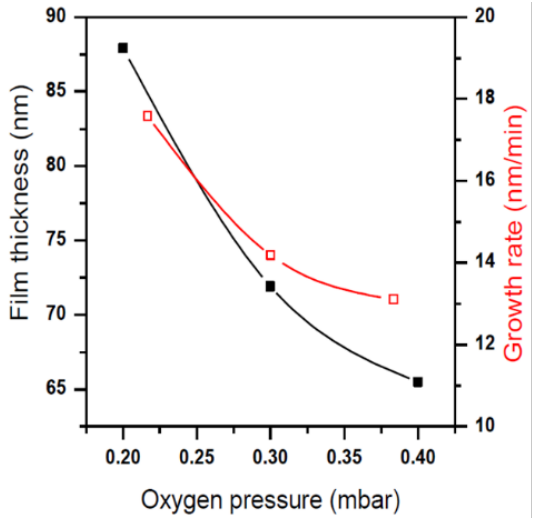

Figure 2. Variation of film thickness and growth rate of P-Cu_2O films as a function OP.

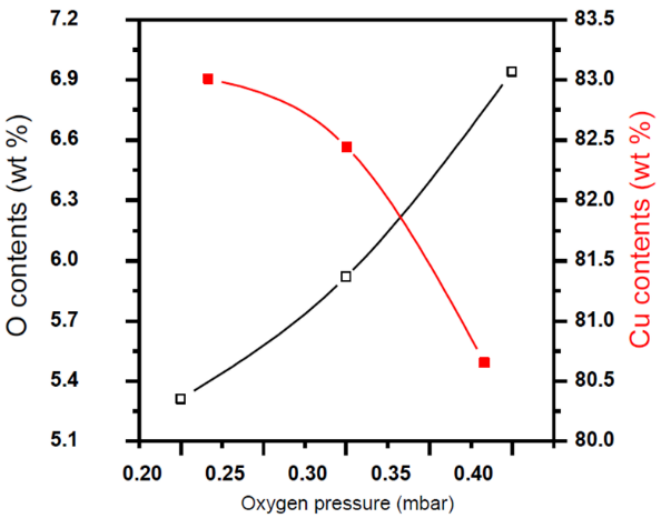

Figure 3. Variation of O and Cu contents in P-Cu_2O films as a function OP.

3.2 Structural Analysis

XRD analysis is used to investigate the various structural parameters like crystallite size (C S), strain (ε), dislocation density (δ), weight fraction $V_{(hkl)}$, d-spacing (d), lattice constant (a), bond length (L), texture coefficients (T C) and number of crystallites per unit area (N_t) of different planes related to Cu_2O films deposited for 0.2, 0.3 and 0.4 mbar OP. The average C S of different planes related to Cu_2O phase is estimated by using the formula[21, 22]:

$$C.S. = \frac{k\lambda}{FWHM cos\theta}$$

where k=0.9 (numeric constant), λ = 1.54 Å (wavelength of incident radiation) and FWHM is the full width at half maximum of the corresponding diffraction peak. The ε developed in different planes of Cu_2O film is estimated by using the relation[23, 24]:

$$\varepsilon = \frac{FWHM cos\theta}{4}$$

The δ is defined as the length of dislocation lines per unit volume of the crystal and is estimated by employing the relation[23, 24]:

$$\delta = \frac{1}{(CS)^2}$$

The weight fraction of Cu_2O (200) and Cu_2O (311) phases is estimated by using the relation[25]:

$$V_{(hkl)} = \frac{I_{(hkl)}}{\sum I_{(hkl)}}$$

where $I_{(hkl)}$ and $V_{(hkl)}$ are the peak intensity and weight fraction of the respective planes of Cu_2O film. The d, a, L, T C and N_t of Cu_2O films are calculated by using the relation[24, 26-28]:

$$2dsin\theta = n\lambda$$

$$a = d\,(h^2 + k^2 + l^2)^{1/2}$$

$$L = 0.6\,a$$

$$TC_{(hkl)} = \frac{I_{(hkl)}/I_{o(hkl)}}{\frac{1}{N}\sum I_{(hkl)}/I_{o(hkl)}}$$

$$N_t = \frac{Film\ thickness}{(Crystallite\ size)^3}$$

where n = 1 and λ is the wavelength of x-rays whereas $I_{(hkl)}$, $I_o(hkl)$, N and N_t are the observed and standard peak intensities, total number of diffraction peaks and total number of crystallites per unit area respectively. The above mentioned equations are used to calculate the different structural parameters like peak intensity, d-spacing, a, cell volume, *C S, δ, T C, ε, N_t, L* and $V_{(hkl)}$ of various phases of P-Cu_2O films and their variation with increasing OP.

Figure 4 shows the XRD patterns of P-Cu_2O films deposited on Cu substrates for 0.2, 0.3 and 0.4 mbar OP. The XRD pattern shows the development of Cu_2O (200) and Cu_2O (311) planes for all OP which confirms the deposition of P-Cu_2O films. The intensity of these diffraction planes strongly depends on the increase of OP. The calculated values of *d-spacing* and "*a*" are found to be 0.210, 0.128 nm and 0.421, 0.425 nm respectively which are close to the reported one (a = 0.427 nm) [1]. The small variation in "a" indicates the creation of defects and microstrains. The change in "a" is responsible to change the other parameters like cell volume and d-spacing with increasing OP. The bond length between the involved species is found to be 0.255 nm. The XRD analysis shows that the evaporated copper species make bond with oxygen molecules instead of atomic oxygen having sufficient energy results in the formation of Cu_2O phase.

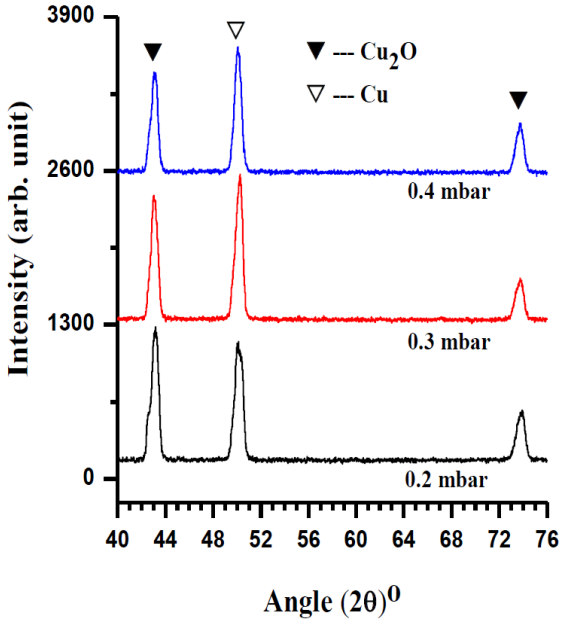

Figure 4. XRD patterns of P-Cu_2O films deposited for 0.2, 0.3 and 0.4 mbar OP**.**

The interpretation of the formation of Cu_2O phase through thermal evaporator can be illustrated by the following chemical equation:

$$2Cu + \frac{1}{2}O_2 \rightarrow Cu_2O$$

The absence of CuO phase (XRD patterns) indicates that the dissociation of oxygen molecules to atomic oxygen does not exist because the evaporation temperature provided to the source material is not sufficient to dissociate the oxygen molecule into atomic oxygen. **Figure 5** reveals the variation in peak intensities of Cu (200), Cu_2O (200) and Cu_2O (311) planes with increasing OP. The change in peak intensity is associated with the increase of OP. The peak intensity of Cu phase is more for 0.3 mbar OP whereas the peak intensities of Cu_2O (200) and Cu_2O (311) planes are greater for 0.2 and 0.4 mbar OP respectively. It means that the ion energy flux available for 0.2 mbar OP is more favorable for the formation of Cu_2O (200) phase whereas the ion energy flux available for 0.4 mbar OP is more suitable for the formation of Cu_2O (311) phase.

Figure 6 reveals the variation in C S of Cu (200), Cu_2O (200) and Cu_2O (311) planes as a function of OP. The average C S of (200) and (311) planes of Cu_2O phase are found to be 19.31, 21.18, 11.32 nm and 22.04, 23.11, 12.08 nm for 0.2, 0.3 and 0.4 mbar OP respectively. The value of C S of all planes is maximum for 0.3 mbar OP whereas it is minimum for 0.4 mbar OP. The defects and microstrains developed in Cu_2O film deposited for 0.3 mbar OP are lower than the defects and microstrains developed in Cu_2O film deposited for 0.4 mbar OP because smaller the crystallite size, greater will be the FWHM and hence defects and microstrains[20].

Figure 7 reveals the variation in ε developed in Cu (200), Cu_2O (200) and Cu_2O (311) planes as a function of OP. The value of ε developed in Cu_2O films deposited for 0.3 mbar OP is minimum whereas it is maximum when the Cu_2O film is deposited for 0.4 mbar OP. This indicates that there is an inverse relation between the C S and ε developed in Cu_2O films.

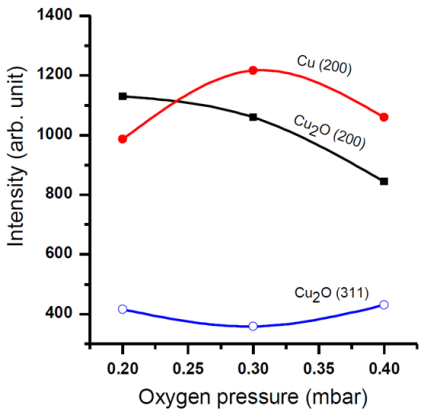

Figure 5. Variations in intensities of different diffraction planes as a function of OP.

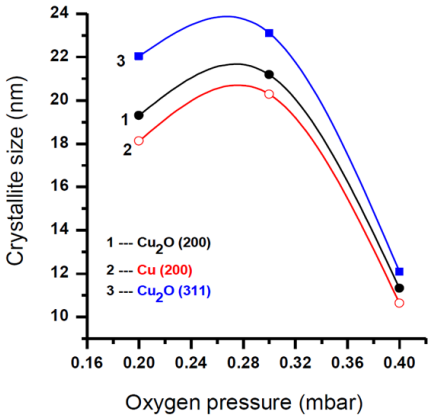

Figure 6. Variations in CS of various diffraction peaks as a function of OP.

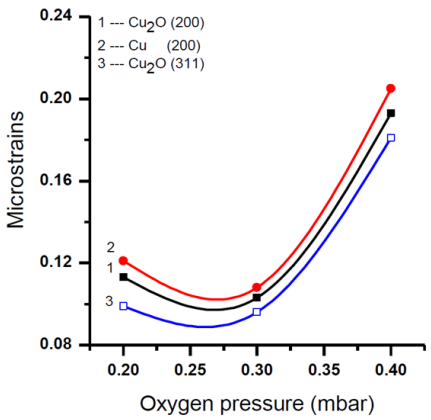

Figure 7. Variation in ε developed in different plans as a function of OP.

Figure 8 reveals the variation in N_t (nm^{-2}) for Cu_2O (200), Cu (200) and Cu_2O (311) planes as a function of OP. The value of N_t are found to be 12.21, 7.46, 45.16; 14.77, 8.5, 54.38 and 8.21, 5.75, 37.16 corresponding to various diffraction planes (mentioned above) with increasing OP respectively. For all OP, the value of N_t is greater for Cu (200) plane which indicates that Cu phase is re-crystallized more thereby indicating the formation of defects and microstrains. It is well known that T C is one of the basic structure parameters in polycrystalline materials which show the crystallization level of deposited film.

Figure 9 shows the T C of Cu_2O (200) and Cu_2O (200) planes developed in P-Cu_2O films deposited for 0.2, 0.3 and 0.4 mbar OP. The value of T C for Cu_2O (200) plane is greater for 0.3 mbar OP whereas it is maximum for Cu_2O (311) plane for 0.4 mbar OP. It means that the Cu_2O (200) phase grows preferentially for 0.3 mbar OP whereas Cu_2O (311) phase grows preferentially for 0.4 mbar OP. It is concluded that the increase in OP plays a vital role to change the preferential growth of P-Cu_2O films. Moreover, the change in T C value is associated with the adatoms kinetic energy of the involved species which is changed with the increase of OP due to change in number of collisions.

Moreover, the change in adatoms kinetic energy of the involved species is associated with the change in substrate surface transient temperature (SSTT), affects the surface energy which is responsible to change the preferential growth of materials like Cu_2O films. It is well known that the change in T C value is attributed with the nucleation of phases,

film surface roughness, development of new crystalline phases in the near vicinity, broaden and asymmetric peaks[29, 30]. **Figure 10** exhibits the variation in weight fraction of Cu_2O phases with increasing OP. The total weight fraction of Cu_2O phases is decreased with the increase of OP. We have already mentioned that the thickness of P-Cu_2O films is decreased with the increase of OP (**Figure 2**). Hence there is a direct relation between the film thickness and weight fraction with the increase of OP.

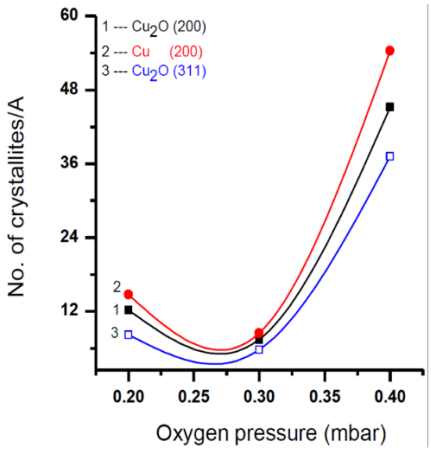

Figure 8. Variation in N_t (nm-2) of various diffraction planes as a function of OP.

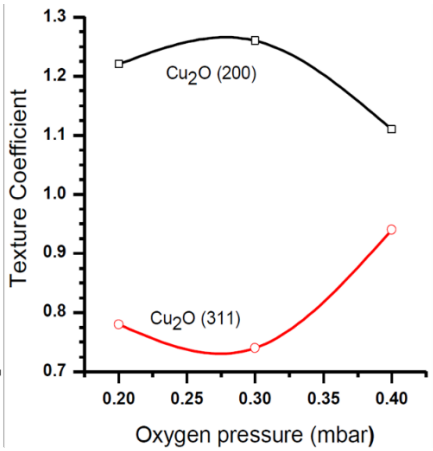

Figure 9. Variation in T C of various planes as a function of OP.

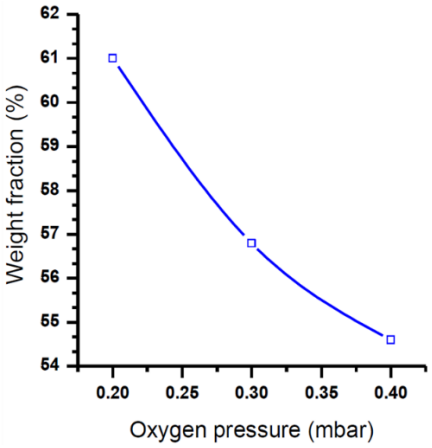

Figure 10. Variation in weight fraction of Cu_2O films as a function of OP.

3.3 SEM Analysis

Figure 11 illustrates the SEM microstructures of P-Cu_2O films deposited for 0.2, 0.3 and 0.4 mbar OP. For 0.2 mbar OP, the SEM microstructure shows the formation of patches of irregular shapes (thickness = ~50 nm) and round- ed nano-particles (size ranged from ~15-20 nm). The distribution of patches of various shapes and rounded nano-particles is uniform which makes the surface compact (outlook appearance). The formation and distribution of various patches, rounded nano-particles and dark or bright regions make the surface rough. For 0.3 mbar OP, the SEM microstructure reveals the formation of clouds of irregular shapes, sliding one above the others, confirming the formation of multi-layers. The formation of dark deep regions and bright hills makes the surface rough. These irregular clouds and their sliding make the surface compact and rough. However, it is difficult to estimate the dimensions of nano-particles forming the irregular clouds and bright hills. For 0.4 mbar OP, the SEM microstructure exhibits the formation of rounded nano-particles of dimensions ranged from 25-150 nm which are distributed uniformly.

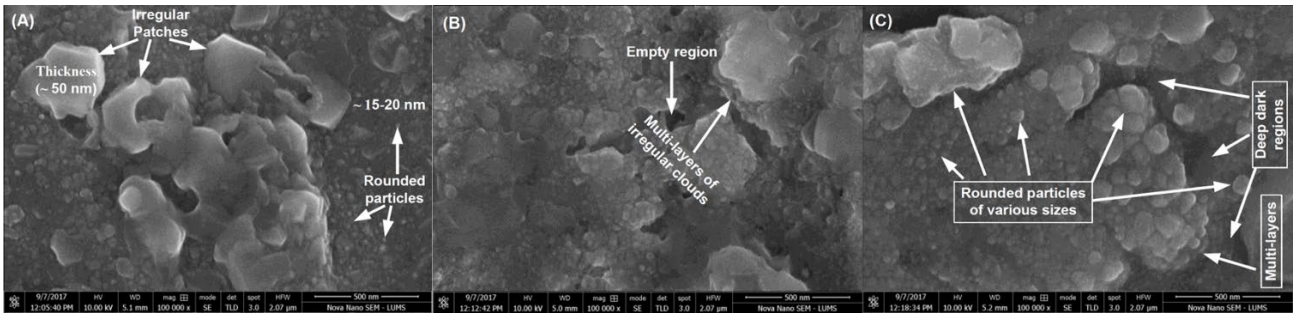

Figure 11. SEM images of P-Cu_2O films deposited for (A) 0.2, (B) 0.3 and (C) 0.4 mbar OP.

The outlook appearance of SEM image shows the formation of cluster of grapes like microstructure which are compact in nature showing uniform distribution. The formation of large hill like particles, containing nano-particles, cluster of rounded grapes and dark deep region make the surface rough. It is concluded that the formation of patches, rounded nano-particles, cluster of grapes and their distribution is associated with the increase of OP. For normal visualization of SEM microstructures, the compact nature of P-Cu_2O films deposited for various OP shows a good adherence to the substrate surface. The changes in surface morphology of P-Cu_2O films are in good agreement with the change in structural parameters. In order to study the optical properties, the Cu_2O films are again deposited on glass substrates for the same deposition parameters.

3.4 Optical Analysis

The optical study of P-Cu_2O films deposited on glass substrates is done viva optical Cauchy model by employing ES and is used to find the optical constants like film thickness (d), refractive index (n), absorption coefficient (α) and optical energy band gap (E_g). We have already discussed the film thickness in section 3.1 which shows that the film thickness is decreased with the increase of OP. **Figure 12** exhibits the variation in n as a function of wavelength. The n of P-Cu_2O films is decreased with the increase of wavelength; however, it strongly depends on the increase of OP.

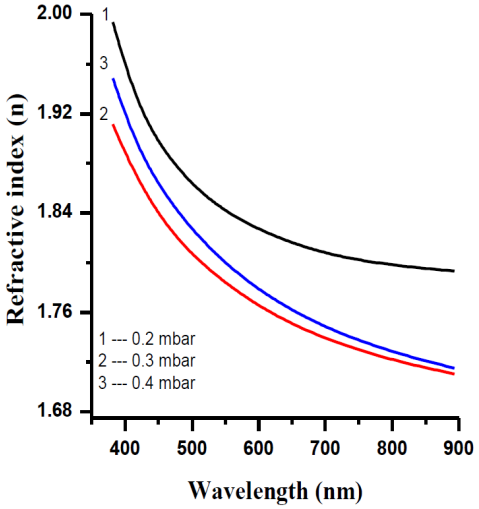

Figure 12. Variation of n values of P-Cu_2O films as a function of wavelengths.

The value of n is greater for 0.2 mbar OP whereas it is smaller for 0.3 mbar OP at all wavelengths. The n values of P-Cu_2O films deposited for 0.2, 0.3 and 0.4 mbar OP are found to be 1.99, 1.91 and 1.94 respectively. This shows that the n of P-Cu_2O films strongly depend on the increase of OP.

Figure 13 exhibits a plot between $(\alpha h\nu)^2$ and photon energy ($h\nu$). The value of E_g of P-Cu_2O films is determined from the value of intercept of the straight line at. It is found that the E_g values of P-Cu_2O films are found to be 2.47, 2.44 and 2.25 eV. This shows that the E_g values are decreased with the increase of OP. Results indicate that the values of n and E_g are maximum for lower (0.2 mbar) OP, however, the values of n and E_g are smaller for 0.3 and 0.4 mbar OP respectively. It is concluded that after 0.2 mbar OP, these values are strongly associated with the increase of OP. It is known that the value of optical absorption is increased with the increase of film thickness which reduces the transmittance. In our case, the film thickness is decreased with the increase of OP. This indicates that the optical absorption of the deposited films is decreased with the increase of OP which enhances the transmittance.

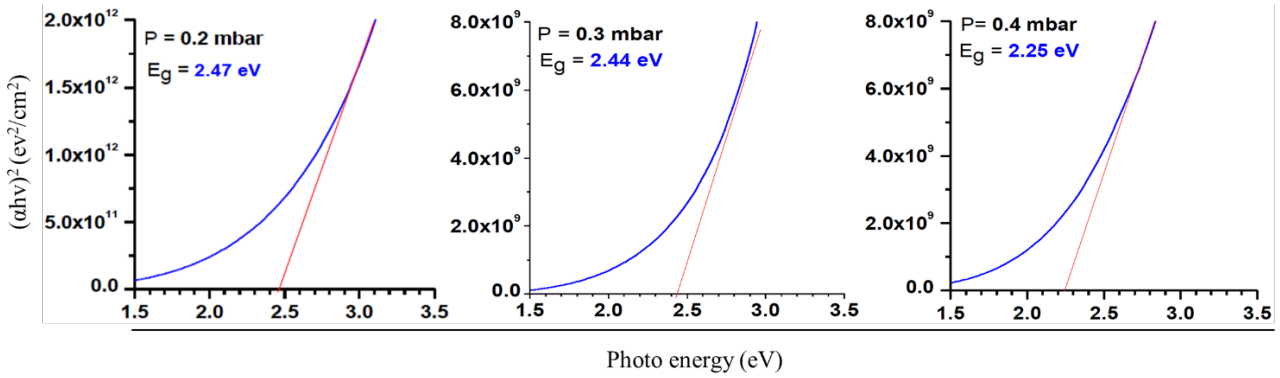

Figure 13; Variation of E_g values of P-Cu_2O films deposited for various OP as a function of photon energy.

Therefore, the P-Cu_2O film deposited for 0.2 mbar OP may act as more optical absorber whereas the P-Cu_2O films deposited for 0.4 mbar OP is more transparent comparatively. It means that the optical transmittance of P-Cu_2O films strongly depends on the increase of OP. It is well known that the E_g value is ranged from 2.0 to 2.6 eV for Cu_2O film whereas it is ranged from 1.3 to 2.1 eV for CuO film depending on the deposition temperature[31-33]. In our case, the E_g

value of copper oxide films ranges from 2.47 to 2.25 eV with increasing OP which confirms the formation of Cu_2O phase only. The formation of CuO or Cu_2O phase depends on the sticking probability which depends on oxygen to Cu flux ratio. In our case, the oxygen to Cu flux ratio is ranged from 0.06 to 0.09 corresponds to 0.2 to 0.4 mbar OP which is sufficient to form Cu_2O phase only because no diffraction peak related to CuO phase is observed (XRD patterns). It means that the dissociation of oxygen molecules in to atomic oxygen does not occur during the deposition process.

In our case, we imagine that the dissociation of oxygen molecules into atomic oxygen may be associated with the evaporation temperature given to the source material. It means that the applied evaporation temperature is not sufficient to dissociate the oxygen molecules into atomic oxygen to Cu_2O phase and hence higher evaporation temperature is needed to dissociate the oxygen molecule into atomic oxygen. It is concluded that a simple and cost-effective thermal evaporator can be used to deposit P-Cu_2O films which is a p-type semiconductor material. The energy band gap of Cu_2O film deposited by thermal evaporator is ranged from 2.25 to 2.47 eV depending on the OP and can be used for solar cell applications.

4. Conclusion

P-Cu_2O films are deposited on Cu substrates for 0.2, 0.3 and 0.4 mbar OP by thermal evaporator. The XRD pattern shows the development of various diffraction planes confirming the deposition of P-Cu_2O films. The intensity of various planes strongly depends on the increasing OP. The C S and ε developed in (200) and (311) planes are found to be 19.31, 21.18, 11.32 nm; 22.04, 23.11, 12.08 nm and 0.113, 0.103, 0.193; 0.099, 0.096, 0.181 with increasing OP respectively. The values of *d-spacing* and α are found to be 0.210, 0.128 nm and 0.421, 0.425 nm respectively. The L of P-Cu_2O film is found to be 0.255 nm. The N_t of the above-mentioned planes is found to be 12.21, 7.46, 45.16 nm^{-2} and 8.21, 5.75, 37.16 nm^{-2} whereas the T C are found to be 1.22, 1.26, 1.11 and 0.78, 0.74 and 0.56 respectively with increasing OP. The O and Cu contents are found to be 5.31, 5.92, 6.94 wt % and 83.01, 82.44, 80.65 wt % respectively. The thickness and growth rate of P-Cu_2O films are found to be 87.9, 71.9, 65.5 nm and 17.6, 14.2, 13.1 (nm/min) with increasing OP respectively. The SEM microstructures reveal the formations of patches of irregular shapes, rounded nano-particles, clouds of nano-particles and their distribution depend on the increasing OP. The n and E_g values of P-Cu_2O films are found to be 1.96, 1.89, 1.92 and 2.47, 2.44 and 2.25 eV with increasing OP respectively. Therefore, the P-Cu_2O films are p-type semiconductor material and can be deposited by a simple and cost-effective thermal evaporator.

Acknowledgement

The authors would like to thanks the Higher Education Commission, Pakistan for proving funds to install thermal evaporator at Thin Films Deposition Lab, Department of Physics, GC University Faisalabad.

References

1. B. Balamurugan, and B. R. Mehta, “Nanocrystalline Thin Films, Optical Properties,Structural Properties, X-Ray Diffraction,” Thin Solid Films, vol. 396, pp. 90-96, 2001.
2. A. Karapetyan, A. Reymers, S. Giorgio, C. Fauquet, L. Sajti, S. Nitsche, M. Nersesyan, V Gevorgyan, and W Marine “Cuprous oxide thin films prepared by thermal oxidation of copper layer, Morphological and optical properties” Journal of Luminescence, vol. 159, pp. 325-332, 2015.
3. J. F. Pierson, A. T. Keck, and A. Billard, “Cuprite, paramelaconite and tenorite films deposited by reactive magnetron sputtering” Appl. Surf. Sci., vol. 210, pp. 359-367, 2003.
4. A. R. Rastkar, A. R. Niknam, and B. Shokri, Characterization of copper oxide nanolayers deposited by direct current magnetron sputtering, Thin Solid Films, vol. 517, pp. 5464-5467, 2009.
5. A. E. Rakshani, “Preparation, characteristics and photovoltaic properties of cuprous oxide; a review” Solid State Electronics, vol. 29, pp. 7-17, 1986.
6. F. Marabelli, G. B. Parraviciny, and F. S. Drioli, “Optical gap of CuO,” Phys. Rev. B, vol. 52, 1433, 1995.
7. J. Ghijsen, L. H. Tjeng, J. V. Elp, H. Eskes, J. Westerink, G. A. Sawatzky, and M. T. Czyzyk, “Electronic structure of Cu2O and CuO,” Phy. Rev. B, vol. 38, pp. 11322, 1988.
8. F. P. Koffyberg, and F. A. Benko, “A photoelectrochemical determination of the position of the conduction and va- lence band edges of p-type CuO,” J. Appl. Phys., vol. 53, pp.1173, 1982.
9. S. Ghosh, D. K. Avasthi, P. Shah, V. Ganesan, A. Gupta, D. Sarangi, R. Bhattacharya, and W. Assmann, Deposition of thin films of different oxides of copper by RF reactive sputtering and their characterization. Vacuum, vol. 57, pp. 377-385, 2000.

10. S. Ishizuka, S. Kato, Y. Okamoto, T. Sakurai, K. Akimoto, N. Fujiwara, and H.Kobayashi, "Passivation of defects in polycrystalline Cu_2O thin films by hydrogen or cyanide treatment," Appl. Surf. Sci., vol. 216, pp. 94-97, 2003.
11. M. Wautelet, A. Roos, and F. Hanus, Optical characteristics of laser-synthesised extended thin films of copper oxide," J. Phys. D: Appl. Phys., vol. 23, pp. 991, 1990.
12. L. S. Huang, S. G. Yang, T. Li, B. X. Gu, Y. W. Du, Y. N. Lu, and S. Z. Shi,"Preparation of large-scale cupric oxide nanowires by thermal evaporation method," J.Cryst. Growth, 260, pp. 130-135, 2004.
13. C. A. N. Fernando, and S. K. Wetthasinghe, "Investigation of photoelectrochemical characteristics of n-type Cu_2O films," Sol. Energy Mater. Sol. Cells, vol. 63, pp. 299-308,2000.
14. L. Armelao, D. Barreca, M. Bertapelle, Y. Bottaro, C. Sada, and E. Tondello, "A sol–gel approach to nanophasic copper oxide thin films," Thin Solid Films, vol. 442, pp. 48-52,2003.
15. T. Mahalingam, J. S. P. Chitra, J. P. Chu, and P. Sebastian, Preparation and microstructural studies of electrode-posited Cu_2O thin films," J. Mater. Lett. Vol. 58, pp.1802-1807, 2004.
16. T. Minami, H. Tanaka, T. Shimakawa, J. Miyata, H. Sato, "High-Efficiency Oxide Heterojunction Solar Cells Using Cu_2O Sheets," Jpn.J. Appl. Phys. Vol. 43, pp. L917,2004.
17. T. Maruyama, "Copper Oxide Thin Films Prepared from Copper Dipivaloylmethanate and Oxygen by Chemical Vapor Deposition," Jpn. J. Appl. Phys. Vol. 37, pp. 4099, 1998.
18. K. Santra, C. K. Sarkar, M. K. Mukherjee, and B. Ghosh, "Copper oxide thin films grown by plasma evaporation method," Thin Solid Films, vol. 213, pp. 226-229, 1992.
19. R. Kita, K. Kawaguchi, T. Hase, T. Koga, R. Itti, and T. Morishita, Effects of oxygen ion energy on the growth of CuO films by molecular beam epitaxy using mass-separated low-energy O+ beams," J. Mater. Res. Vol. 9, pp. 1280-1283, 1994.
20. I. A. Khan, M. Noor, A. Rehman, A. Farid, M. A. K. Shahid, and M. Shafiq, "Role of evaporation time on the structural and optical properties of ZnO films deposited by thermal evaporator," Eur. Phys. J. Appl. Phys., vol. 72, pp. 30302, 2015.
21. G. K. Williamson, and R. E. Smallman, "Dislocation densities in some annealed and cold-worked metals from measurements on the X-ray debye-scherrer spectrum," Philosophical Magazine vol. 1, pp. 34-46, 1956
22. X. S. Wang, Z. C. Wu, J. F. Webb, and Z. G. Liu, "Ferroelectric and dielectric properties of Li-doped ZnO thin films prepared bypulsed laser deposition," Appl. Phys.A, vol. 77, pp. 561-565, 2003.
23. Z. R. Khan, M. Zulfequar, and M. S. Khan, "The Effect of ZnO Thin Film and Its Structural and Optical Properties Prepared by Sol-Gel Spin Coating Method," Mat. Sci. &Engg. B, vol. 174, 145-149, 2010.
24. Z. R. Khan, M. S. Khan, M. Zulfequar, and M. S. Khan, „Optical and structural properties of ZnO thin films fabricated by sol-gel method," Mat. Sci. & Appl., vol. 2, pp. 340-345,2011.
25. E. Djurado, P. Bouvier, and G. Lucazeau, "Crystallite Size Effect on the Tetragonal-Monoclinic Transition of Undoped Nanocrystalline Zirconia Studied by XRD and Raman Spectrometry," J. of Solid State Chemistry, vol. 149, pp. 399-407, 2000.
26. B. D. Cullity, and S. R. Stock, Elements of X-ray Diffraction. Prentice Hall, New Jersey,2001.
27. R. Mariappan, M. Ragavendar, and V. Ponnuswamy, "Growth and characterization of chemical bath deposited Cd1−x ZnxS thin films," J. Alloys Compd., vol. 509, pp. 7337-7343, 2011.
28. M. H. Mamat, M. Z. Sahdan, Z. Khusaimi, A. Z. Ahmed, S. Abdulah, and M. Rusop, "Influence of doping concentrations on the aluminum doped zinc oxide thin films properties for ultraviolet photo conductive sensor applica- tions," Opt. Mater., vol. 32, pp. 696-699, 2010.
29. A. Rizzo, M. A. Signore, M. F. D. Riccardis, L. Capodieci, D. Dimaio, and T. Nocco, "Influence of growth rate on the structural and morphological properties of TiN, ZrN and TiN/ZrN multilayers," Thin Solid Films, vol. 515, pp. 6665-6671, 2007.
30. I. A. Khan, M. Hassan, T. Hussain, R. Ahmad, M. Zakaullah, and R. S. Rawat,"Synthesis of nano-crystalline zirconium aluminium oxynitride (ZrAlON) composite films by dense plasma Focus device," Applied Surface Science, vol. 255, pp. 6132-6140,2009.
31. F. K. Mugwang'a, P. K. Karimi, W. K. Njoroge, O. Omayio, and S. M. Waita, Optical characterization of Copper Oxide thin films prepared by reactive dc magnetron sputtering for solar cell applications," Int. J. Thin Film Sci. Tec., vol. 2, pp. 15-24, 2013.
32. K. Kawaguchi, R. Kita, M. Nishiyama, and T. Morishita, "Molecular beam epitaxy growth of CuO and Cu_2O films with controlling the oxygen content by the flux ratio of Cu/O". Journal of Crystal Growth vol. 143, pp. 221-226, 1994.
33. K. P. Muthe, J. C. Vyas, S. N. Narang, D. K. Aswal, S. K. Gupta, D. Bhattacharya, R.Pinto, G. P. Kothiyal, and S.C. Sabharwal, "A study of the CuO phase formation during thin film deposition by molecular beam epitaxy," Thin Solid Films, vol. 324, pp. 37-43,1998.